THE USE OF METEOROLOGICAL PARAMETERS FOR A REGULATORY DIAGNOSTIC MODEL PERFORMANCE EVALUATION FOR HOUSTON, TEXAS

Tamara Paris-Davila

A thesis submitted to the faculty at the University of North Carolina at Chapel Hill in partial fulfillment of the requirements for the degree of Master of Science in the Department of Environmental Sciences and Engineering in the Gillings School of Global Public Health.

Chapel Hill
2022

Approved by:

William Vizuete

Barron Henderson

Jason West

ABSTRACT

Tamara Paris-Davila: The use of meteorological parameters for a regulatory diagnostic model performance evaluation for Houston, Texas
(Under the direction of William Vizuete)

This study presents a meteorological process-based evaluation of a regulatory model that was approved by the Environmental Protection Agency for developing ozone (O_3) control strategies for the Houston-Galveston-Brazoria (HGB) non-attainment region. This evaluation used metrological parameters that were strongly correlated with observed O_3 exceedance days: degree of wind rotation, morning wind speeds, and midnight wind direction. The model overpredicted days with low wind rotations and underpredicted days with high wind rotations. Model predicted morning wind speeds consistently reached levels twice that of observations and the midnight wind directions were also rarely simulated correctly. These predicted differences in meteorological processes highlighted in this study could lead to different influence of emission sources and the location of peak O_3 concentrations. Because these meteorological processes are correlated with O_3 in HGB, correctly simulating them would reduce uncertainty in O_3 predictions and provide more confidence in the representativeness for the development of control strategies.

TABLE OF CONTENTS

LIST OF TABLES

Table

LIST OF FIGURES

LIST OF ABBREVIATIONS

AQM	Air Quality Model
BAYP	Bayland Park
CAMS	Continuous Ambient Monitoring Stations
CAMx	Comprehensive Air Quality Model with Extensions
DPK2	Deer Park #2
DV	Design Value
EPA	Environmental Protection Agency
HALC	Aldine
HGB	Houston-Galveston-Brazoria
LJKS	Lake Jackson
LST	Local Standard Time
MACP	Manvel Croix Park
MOVES	Motor Vehicle Emissions Simulator
MPE	Model Performance Evaluation
NAAQS	National Ambient Air Quality Standard
O_3	Ozone
PPB	Parts Per Billion
RMSE	Root Mean Square Error
RRF	Relative Response Factor
SBFP	Seabrook Friendship Park
SIP	State Implementation Plan

TCEQ	Texas Commission on Environmental Quality
WRF	Weather Research and Forecasting

INTRODUCTION

Due to the known adverse effect of ozone (O_3) on human health (EPA, n.d.-a), O_3 is regulated by the Environmental Protection Agency (EPA) with a National Ambient Air Quality Standard (NAAQS). Based on this O_3 standard, an area is designated as attainment or nonattainment by using the annual fourth-highest daily maximum 8-hour concentration averaged over 3 years (EPA, n.d.-b). If attainment is not met, the geographic area is required to submit a state implementation plan (SIP) to the EPA that includes mitigation strategies. To prove the efficacy of these mitigation strategies, it is federally mandated that a photochemical air quality model (AQM) is used. Therefore, these AQMs must have sufficient model performance to assess whether future control strategies will provide attainment of the NAAQS. To assess model performance, the EPA has developed and recommends the use of strategies described in their model performance evaluation (MPE) framework (EPA, 2014).

The MPE framework includes four approaches, shown in Table 1, that are considered appropriate for evaluating AQMs (EPA, 2014). According to the MPE framework, the minimum requirement for an attainment demonstration is an operational evaluation using all available ambient monitoring data for the model simulation period (EPA, 2014). This requires the use of statistical performance metrics of hourly and 8-hour time averaged concentrations of O_3 for each day of the model simulation when values are over 60 ppb. The metrics in an operational evaluation include statistical bias, error, and graphical displays such as time series. Operational evaluations provide insufficient evidence to conclude whether or not an AQM's "good"

performance was the result of accurate science, or the product of compensating errors known as equifinality (Beven & Freer, 2001). Compensating errors could occur for various reasons, for example a model may overestimate emissions or background concentrations while having very disperse meteorology therefore causing both errors to compensate for each other. In this scenario, an operational evaluation would show good performance, but this good performance would be due to incorrect processes the operational evaluation could not detect. Although operational metrics are critical for a MPE, the use of diagnostic parameters can provide insights on whether the model processes are producing the predicted concentration for the right reason.

Table 1. Environmental Protection Agency's model performance evaluation (MPE) approaches for attainment demonstration (EPA, 2014).

MPE Framework Approach	**Approach Characteristics**
Operational	Includes statistical and graphical analyses aimed at determining whether the modeled simulated variables are comparable to measurements.
Diagnostic	Focuses on process-oriented analyses that determine whether the individual processes and components of the model system are working correctly, both independently and in combination.
Dynamic	Assesses the ability of the air quality model to predict changes in air quality given changes in source emissions or meteorology.
Probabilistic	Attempts to assess the level of confidence in the model predictions through techniques such as ensemble model simulations.

The Houston-Galveston-Brazoria (HGB) region is an example of an O_3 non-attainment region that features the complex interplay of emission sources and complex meteorology that could lead to compensating errors (Murphy & Allen, 2005; Nam et al., 2006). Since 2000, the Texas Commission on Environmental Quality (TCEQ) has submitted five SIPs (supplemental table 1) and currently HGB is designated as a marginal nonattainment area of the 2015 70 ppb

eight-hour O_3 NAAQS, and a serious nonattainment area of the 2008 75 ppb eight-hour O_3 NAAQS. The two SIPs submitted by the TCEQ pertaining to the 75 ppb eight-hour O_3 NAAQS use a 2012 base year for their air quality model. The TCEQ completed an operational evaluation of this model, and the EPA approved it for use in developing regulatory strategies. It is important to note that the SIP evaluations were solely operational, cited by the TCEQ as due to a lack of time. Operational analysis was completed for all monitors from May to September 2012 and are publicly available (TCEQ, 2020a, 2020b). Figure 1 shows the one-hour O_3 bias comparison for observed $O_3 \geq 60$ ppb and includes reference lines of model performance from other relevant models. The O_3 bias for one-hour O_3 was either below or around the same O_3 bias (less than 5 ppb) found for comparable models. The root mean square error (RMSE) was always either below or around the same RMSE found for comparable models; 18 ppb for one-hour O_3 and 14 ppb for eight-hour O_3 (TCEQ, 2020a). O_3 bias was much higher when compared to other models' bias but when narrowed down to only observed values ≥ 60 ppb the bias was still comparable to other models. Overall, the TCEQ reported that the model was considered suitable for reaching attainment goals (TCEQ, 2020a).

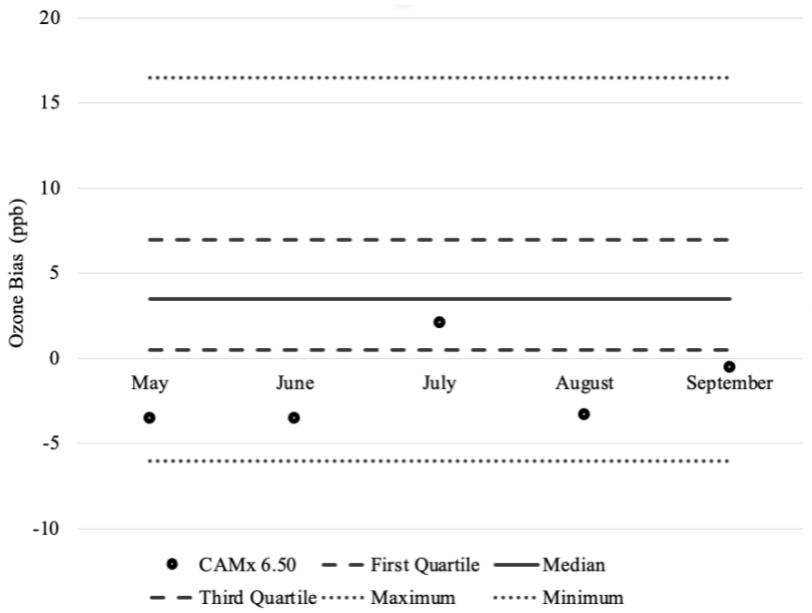

Figure 1. The TCEQ SIP reported 2012 one-hour ozone bias by month for observations ≥ 60 ppb in the Houston-Galveston-Brazoria (HGB) area (TCEQ, 2020b). Reference lines are compiled ozone bias performance statistics for 69 regional air quality model runs from 2006-2012 (Simon et al., 2012).

In addition to considerable modeling resources, the HGB meteorology has also been subject to significant investigation. Research has found that since the HGB region is located on the Gulf of Mexico, coastal wind flows are subject to a diurnally changing temperature gradient and synoptic forces that combine to create specific O_3 conducive conditions (Banta et al., 2011; Li et al., 2020; Vizuete et al., In Press). Part of these synoptic forces is the Coriolis force which causes a complete 360-degree wind rotation to occur every 24 hours at Houston's latitude of 30 degrees (Vizuete et al., In Press). Using cluster techniques and data from the Texas Air Quality Studies, studies presented that high O_3 was related to clusters representing the Gulf breeze (Banta et al., 2011; Darby, 2005). Another study used cluster techniques to associate high O_3 concentration in Houston with sea-breeze-driven wind rotation and recirculation (Li et al., 2020). This sea-breeze-driven wind rotation and recirculation consisted of a clockwise wind rotation throughout the day and light morning wind speeds that get progressively stronger throughout the day; the high O_3 was attributed to pollution recirculation and stagnation. On the other hand, the

study also found lowest 8-hour O_3 occurring when there were strong winds from the south direction bringing in clean marine air which allowed for dissipation of pollution (Li et al., 2020).

A previous study by Vizuete et al. (In Press) used 15 years of O_3 and wind data to identify specific meteorological parameters associated with observed O_3 exceedance days. Wind vector data was compared for O_3 exceedance days, 4,375 monitor days, and non-exceedance days, 94,853 days. Their research describes a typical O_3 conducive day as a day with morning winds generally from the northwest that move HGB emissions into the Gulf of Mexico. The regional winds then begin to rotate until by 06:00 local standard time (LST) they are blowing from the southeast and those emissions in the Gulf are reintroduced over HGB. It is during this rotation where some of the lowest wind speeds of the day are observed between 00:00-06:00 LST. Once the wind direction has fully rotated from the northwest to the southeast the wind speeds across HGB accelerate and flow out towards the west or northwest of HGB. It is at monitors in north and west HGB where some of the highest O_3 is observed. For example, the monitor furthest north in this study, Aldine (HALC), has had some of the highest design values for the past 5 years. In contrast, a non-ozone conducive day, as described in the literature (Vizuete et al., In Press), would have a consistent wind direction and does not feature a rotation in wind direction and thus adverting emissions from HGB in one direction. Wind speeds on this day also are higher than a day featuring rotation and lacks that window of lower wind speeds between 00:00 – 06:00 LST.

The study also used a simple mixed layer sea-breeze model to recreate observed wind trajectories for the HGB area. This model was capable of reproducing the meteorological conditions caused by a diurnally changing temperature gradient and synoptic forces that would be observed at a stationary surface monitor in HGB. At a stationary surface monitor the O_3 conducive meteorology would feature a wind rotation across all four quadrants of a compass

throughout the day, a significant decrease in wind speeds in the morning hours and a midnight wind direction from the northwest (Vizuete et al., In Press). This previous work identified metrological processes correlated with high O_3 through monitor observations but no work was done to evaluate whether these same processes are occurring within a regulatory O_3 model. The following work describes the application of these observed O_3 conducive parameters with a HGB regulatory model that has sufficiently passed an operational evaluation to reveal any insights on whether the model correctly predicted these meteorological processes that led to high O_3. If these processes are not predicted then uncertainty is introduced on the findings of the operational model performance, and ultimately the O_3 mitigation strategies which are based on those predictions.

METHODS

Air Quality Modeling Data

This study relied on the Comprehensive Air Quality Model with Extensions (CAMx) version 6.50 (Ramboll Environ, 2016) as described in the TCEQ's latest SIP for the HGB region and the TCEQ website (TCEQ, 2020b). The modeling period was from May through September 2012 and uses the Carbon Bond 6 "revision 4" gas-phase chemistry mechanism with condensed halogen chemistry and inline sea salt emissions (TCEQ 2020). Meteorological inputs were generated with the Weather Research and Forecasting (WRF) model. For the 36 km domain, the TCEQ developed the land use file using version 3 of the Biogenic Emissions Land use Database for areas outside the U.S. and the 2006 National Land Cover Dataset for the U.S. For the 4 km and 12 km domains, the TCEQ used updated land-use files developed by Texas A&M University (TCEQ, 2020b).

The EPA's 2011 Modeling Platform, Air Markets Program Data, the State of Texas Air Reporting System and local inventories provided the major inputs for the stationary emission source types. On road mobile source emissions were derived from vehicle miles traveled activity combined with emission rates from the EPA's Motor Vehicle Emissions Simulator (MOVES) model. Non-road mobile source emissions came from the Texas NONROAD model and MOVES. Biogenic emissions came from version 3.61 of the Biogenic Emission Inventory System. Stationary, on-road, non-road, and off-road emission estimates were put into the model by using version three of the Emissions Processing System (TCEQ, 2020b).

Observational Data

Observational data was collected from regulatory Continuous Ambient Monitoring Stations (CAMS) operated by the TCEQ. The locations of these monitors can be found in Figure 2 and supplemental table 2. The observed data were collected from May to September 2012. The 2012 CAMS observed data included hourly air quality data for O_3 and meteorological variables such as wind direction and speed. The TCEQ oversees monitoring ambient air concentrations at stationary monitoring sites across the state. Location of these monitors is determined by federal air monitoring rules and to ensure quality of monitoring data the TCEQ uses a variety of measures. Monitoring instruments meet federal sampling and analytical requirements. A validation assessment is also performed on all data to verify that the TCEQ's data quality objectives are met. Data are reviewed for outliers, regional comparability, quality assurance/quality control requirements, and other data quality assessment indicators (TCEQ).

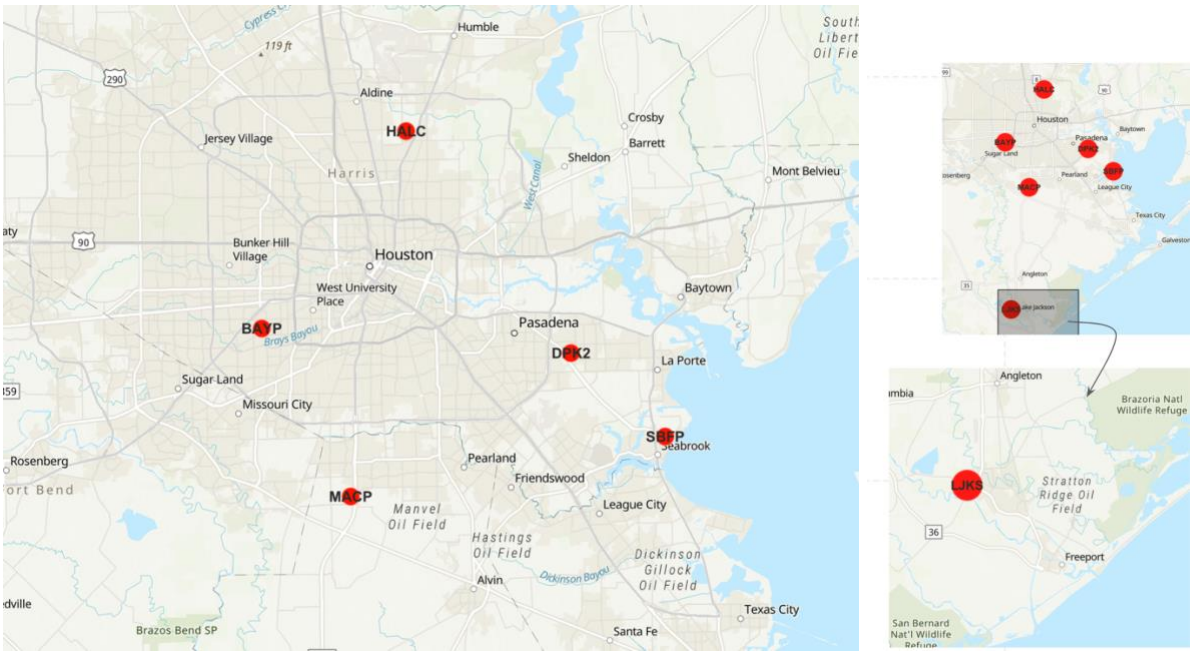

Figure 2. Locations of monitors used for analysis. Manvel Croix Park (MACP), Deer Park #2 (DPK2), Bayland Park (BAYP) and Aldine (HALC) are inland monitors. Lack Jackson (LJKS) and Seabrook Friendship Park (SBFP) are coastal monitors.

Six monitors were selected for this analysis (Figure 2). Four of these were inland monitors with different geographic locations within the HGB area; Manvel Croix Park (MACP)-south, Aldine (HALC)-North, Bayland Park (BAYP)- west and Deer Park #2 (DPK2)- east. MACP is around 25 km south of the Houston core and HALC is around 16 km north from the core while BAYP and DPK2 are aligned around 10 km south of the core in the southwest and southeast directions respectively. The MACP monitor was chosen because it was critical for the HGB area's attainment demonstration due to having the highest design value (DV) in the 2012 modeling year, as seen in Figure 3. In recent years MACP's DV has decreased while other monitors' DV have increased, as shown in Figure 3 (TCEQ, 2021). HALC, BAYP, and DPK2 were chosen because they had the three highest DVs in 2020. Inland monitors are vital for attainment demonstrations therefore making these monitors important to analyze. Two coastal monitors were also chosen: Lake Jackson (LJKS) and Seabrook Friendship Park (SBFP). LJKS is on the coast south of MACP and SBFP is on the coast east of MACP and data from these monitors were chosen to assess the spatial variability in model performance the coastal monitors.

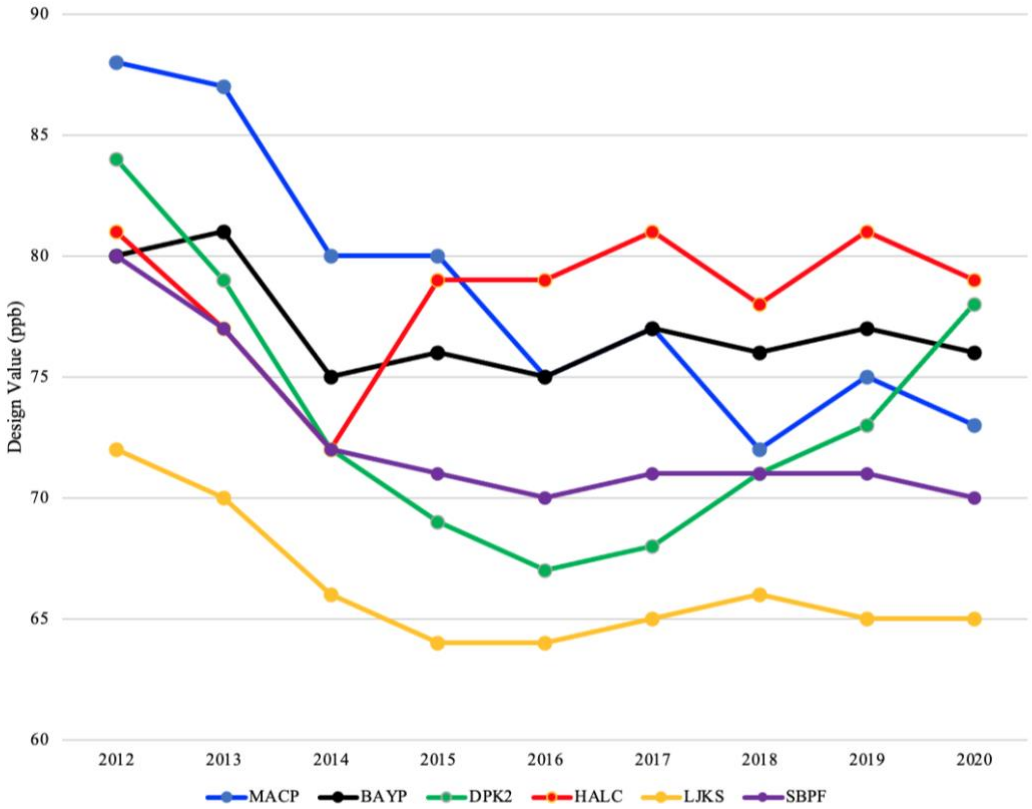

Figure 3. Monitor design values (DV) for Manvel Croix Park (MACP), Bayland Park (BAYP), Deer Park #2 (DPK2), Aldine (HALC), Lake Jackson (LJKS), and Seabrook Friendship Park (SBFP) from years 2012-2020 (TCEQ, 2021).

Meteorological Parameters

This diagnostic performance evaluation will investigate the model's ability to replicate the processes that produce O_3 conducive meteorological conditions. Based on Vizuete et al. (In Press), strong correlations were found with the distribution of rotating winds, the wind speeds during the morning hours, and the midnight wind direction. This analysis paired predicted with observed O_3 and wind data for the modeling period of May to September 2012 and focused on the monitors with the highest DVs and providing spatial coverage of the HGB region.

The distribution of rotating winds is represented by hourly wind direction at each monitor. For each site and day, the distribution is characterized by the number of 90-degree compass quadrants (N:W, N:E, S:E, S:W) occupied by any hour. A 1-quadrant (1Q) day would

be a day when the wind vector only goes through one 90-degree quadrant while a 4Q day would be a day where the wind vector goes through all 90-degree quadrants. 1Q days would represent days with less wind rotation while 4Q days would represent more wind rotation occurring throughout the day. Note that a 2Q or 3Q day includes any combination of quadrants and no effort is made to differentiate between quadrants.

The morning wind speeds will be characterized using the "morning transport distance." Morning transport distance is defined as the approximate distance traveled by an air parcel from a monitor from 00:00 to 06:00 LST. The observed morning transport distance was calculated by summing the resultant wind speeds for hours 00:00 to 06:00 LST. The model values were produced by converting the hourly U and V at each site to wind speed and then the magnitude of wind speeds was summed from hours 00:00 to 06:00 LST. Midnight wind direction was compared from the model and observations. The observation uses the resultant direction from 00:00 to 01:00 LST. The model values were produced by converting the 00:00 LST U and V at each site to wind direction. The wind observations were made from 5-minute averages, while the model used instantaneous points corresponding to the grid cell a monitor is in.

RESULTS

Rotation of Wind Direction

Figure 4 shows, for the MACP and DPK2 monitors, the eight-hour exceedances and the number of 90-degree quadrants (1Q-4Q) the wind vector originated from between midnight to the following midnight. In Figure 4 the observational data show most days being 3Q days with few days being 1Q. In contrast, the regulatory model predicted that the majority of days were 2Q days with relatively fewer 4Q days. This is similar to the results for the BAYP and HALC monitors shown in Figure 5 where model predictions show majority of days being 2Q days. All inland monitor observations showed 3Q and 4Q days being over 50% of the observations which was not seen in the predictions. For example, MACP observations show 68.8% of days as 3Q or 4Q days while model predictions show only 34% of days as 3Q or 4Q days, an underprediction of 34.8%. As for the DPK2 monitor, the 3Q and 4Q days were underpredicted by 26.1%. BAYP and HALC monitor's 3Q and 4Q days were underpredicted by 24.8-26.2%. Overall, for all monitors it is evident that 3Q and 4Q days are underpredicted while 1Q and 2Q days are overpredicted.

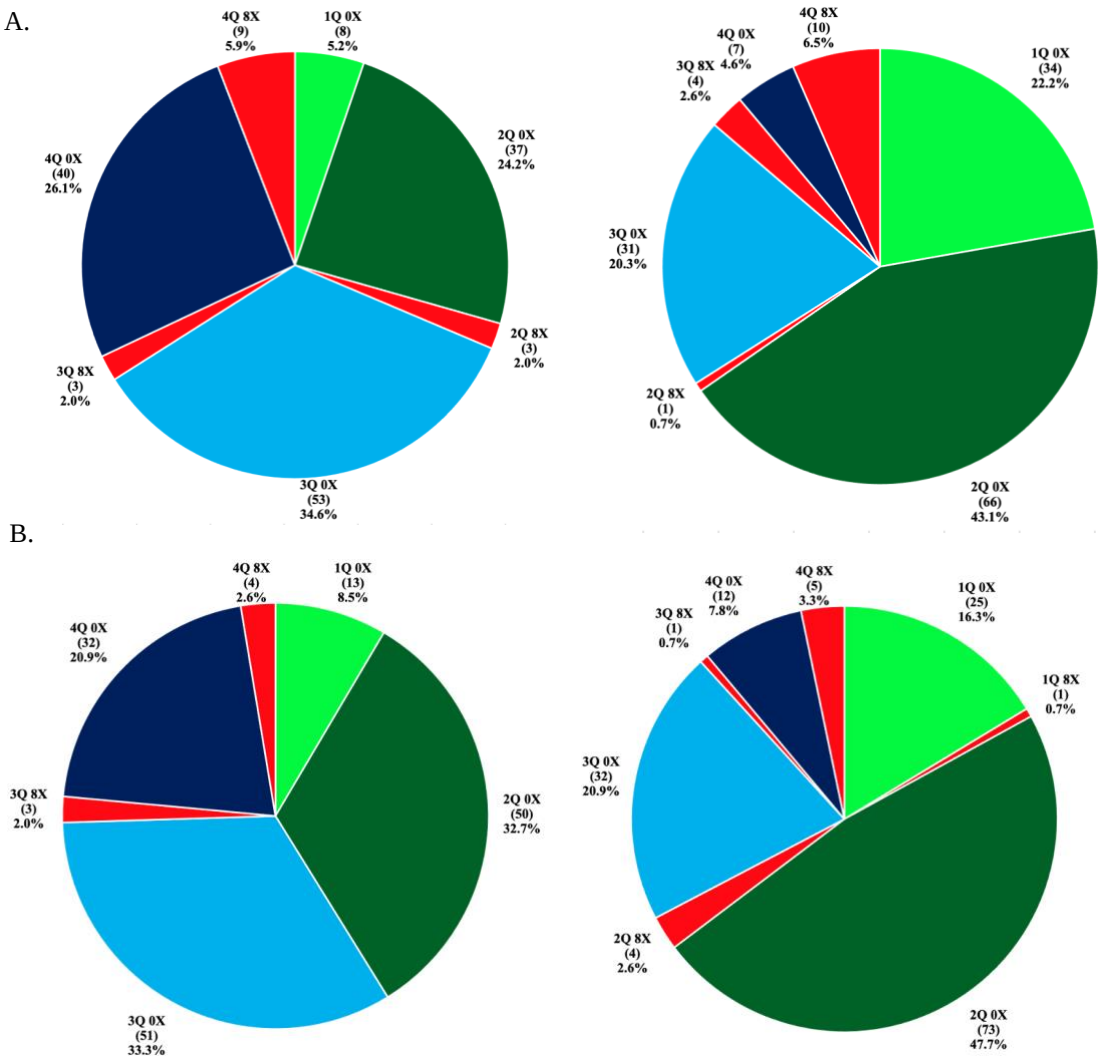

Figure 4. For the (A) Manvel Croix Park (MACP) and (B) Deer Park #2 (DPK2) monitors, the 8-hour quadrant exceedances (8X) and non-exceedances for the 153-day modeling period of May to September for observed (left) and model predictions (right). These quadrants(1Q-4Q) coincide with the number of compass 90-degree quadrants the wind vector originated from between midnight to the following midnight (N:E, E:S, S:W, W:N). 0X days are days with O3 8H < 70 ppb and 8X days are days with O_3 8H >= 70 ppb.

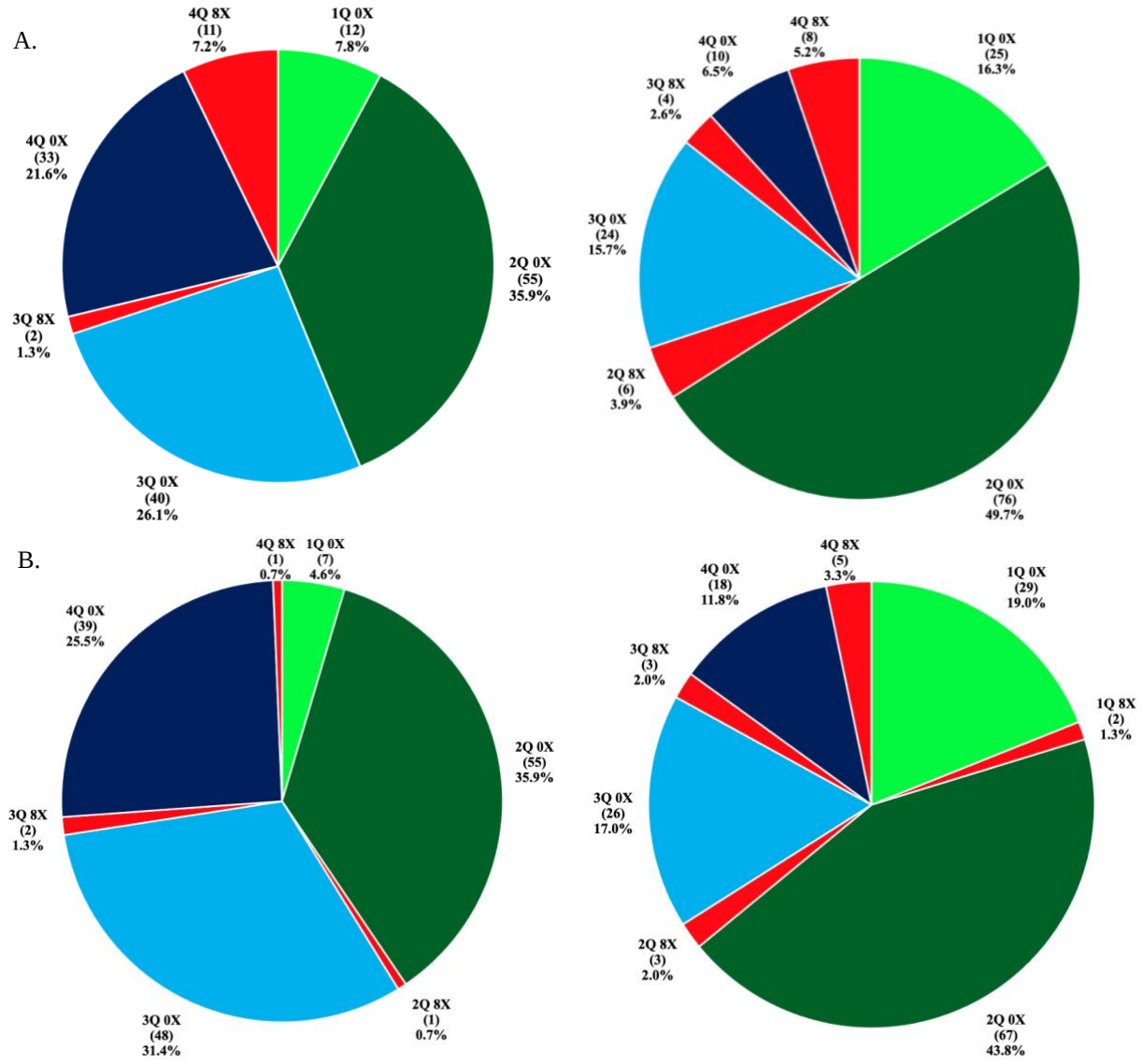

Figure 5. For the (A) Bayland Park (BAYP) and (B) Aldine (HALC) monitors, 8-hour quadrant exceedances (8X) and non-exceedances for the 153-day modeling period of May to September for observed (left) and model predictions (right). These quadrants(1Q-4Q) coincide with the number of compass 90-degree quadrants the wind vector originated from between midnight to the following midnight (N:E, E:S, S:W, W:N). 0X days are days with O3 8H < 70 ppb and 8X days are days with O_3 8H >= 70 ppb.

Figure 6 shows quadrant types and exceedances for the coastal monitors of LJKS and SBFP. The majority of observed LJKS days are 4Q days while the majority of observed SBFP days are 2Q days. For both monitors the model predicts majority of days being 2Q days. LJKS 2Q days were overpredicted by 30.7% and SBFP monitor 2Q days were overpredicted by 7.9%.

As for the 4Q days, the LJKS monitor days were underpredicted by 26.1% and the SBFP days were underpredicted by 10.4%. Despite differing geographically, the pattern of overprediction of 1Q and 2Q days and underprediction of 3Q and 4Q days was also seen within these two monitor locations. The observed LJKS quadrant frequencies were most like the observed MACP monitor frequencies, likely because both monitors are further south in relation to other monitors. Observed SBFP quadrant frequencies were most similar to the observed DPK2 frequencies which can be attributed to their geographical proximity to each other. These results show that quadrant frequency varies based on geography and the model may not be emulating the geographical differences seen in the observations.

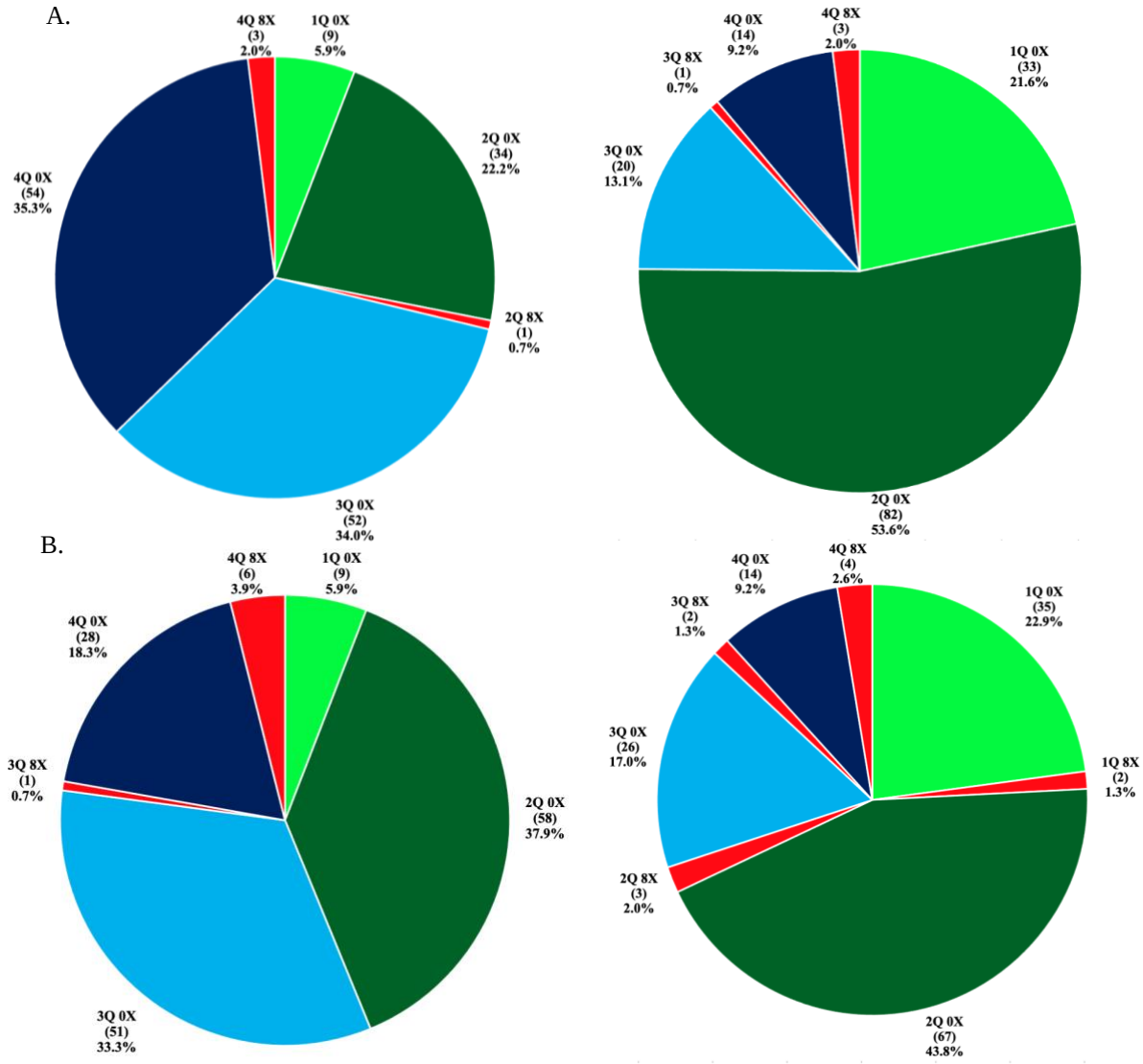

Figure 6. For the (A) Lake Jackson (LJKS) and (B) Seabrook Friendship Park (SBFP) monitors, 8-hour quadrant exceedances (8X) and non-exceedances for the 153-day modeling period of May to September for observed (left) and model predictions (right). These quadrants(1Q-4Q) coincide with the number of compass 90-degree quadrants the wind vector originated from between midnight to the following midnight (N:E, E:S, S:W, W:N). 0X days are days with O3 8H < 70 ppb and 8X days are days with O_3 8H >= 70 ppb.

Wind Rotation and Ozone

All inland monitors but HALC had majority observed and predicted exceedances occur during 4Q days. The model predicated majority of exceedances occurring on 4Q days for these

monitors but overpredicted their frequency. For example, the MACP monitor observations had 5.9% of days as 4Q exceedances while the model predicted 6.5% of days as 4Q exceedances. Along with overpredicting 4Q exceedance days the model predicted various exceedances occurring on 1Q or 2Q days for all monitors, which was rarely observed. Observations showed all of the BAYP monitor's exceedance days occurred during 3Q or 4Q days. In contrast, the model predicted 6 of the 18 predicted exceedances occurring on 2Q days. The HALC monitor observations showed 1 4Q exceedance, 2 3Q exceedances and 1 2Q exceedance; the model overpredicted the number of exceedance days for all these quadrants and predicted exceedances occurring on 1Q days which never occurred in the observations. While the model predicted exceedances occurring more frequently during 3Q or 4Q days it failed to predict the correct frequency of these occurrences and predicted exceedances during 1Q and 2Q days which did not exist. The model's constant underprediction of 3Q and 4Q days while simultaneously predicting the majority of exceedances on these days leads to the prediction of fewer O_3 conducive days. This suggests that when these O_3 conducive days do occur, they are more likely to create exceedance days which is not seen in the observations since there is a large frequency of 3Q and 4Q days occurring without observed exceedances.

For the LJKS monitor, 3 4Q exceedances and 1 2Q exceedance were observed. The model accurately predicted the 4Q exceedances but predicted a 3Q rather than a 2Q exceedance. All but one observed exceedance for the SBFP monitor occurred during a 4Q day (7 days). In contrast, the model showed 4 4Q exceedance days, 2 3Q exceedance days, 3 2Q exceedance days and 2 1Q exceedance days. Similar to what was seen for the inland monitors, exceedances were more likely to occur on 4Q days and although the model predicted more exceedances occurring during 4Q days it still predicted exceedances occurring on quadrants that had no observed

exceedances. For all monitors, there were patterns of overprediction of 1Q and 2Q days and underprediction of 3Q and 4Q days. Along with this, more exceedances were observed to occur on 3Q and 4Q days which coincide with days that had more rotation of winds throughout the day.

For all monitors and for each quadrant type, the observed and predicted O_3 concentration values were determined. Figure 7 shows box plots for the MACP monitor quadrants and exceedance/non-exceedance O_3 concentrations, the rest of the monitors are shown in Supplemental Figures 1-3. The MACP monitor box plots show the non-exceedance day O_3 averages being overpredicted by 10-30 ppb with the 4Q days having the highest overpredictions. This overprediction of non-exceedance day O_3 is seen in all other monitors as well, for example, both BAYP and HALC showed overpredictions of O_3 averages by 12-25 ppb. For all but one inland monitor, the 4Q modeled non-exceedance days had ranges of ~10 ppb which was unlike the observed 4Q non-exceedance days which had ranges of over 40 ppb for all monitors. All monitors showed that the model was unable to predict the lowest and highest observed O_3. The minimums for all quadrants reach concentrations below 20 ppb in the observations. The model predictions on the other hand always had minimum O_3 above 20 ppb for all quadrants. High O_3 was underpredicted by the model, as seen for the MACP monitor, the observed O_3 exceedances reached concentrations over 85 ppb while the model only predicted exceedances to be between 70-80 ppb. The DPK2 monitor and the coastal monitors also showed that the model underpredicted high O_3 as well. Overall, the model overpredicts the non-exceedance day concentrations, fails to capture the range of O_3 concentrations that is seen in the observations and frequently underpredicts high O_3 concentrations.

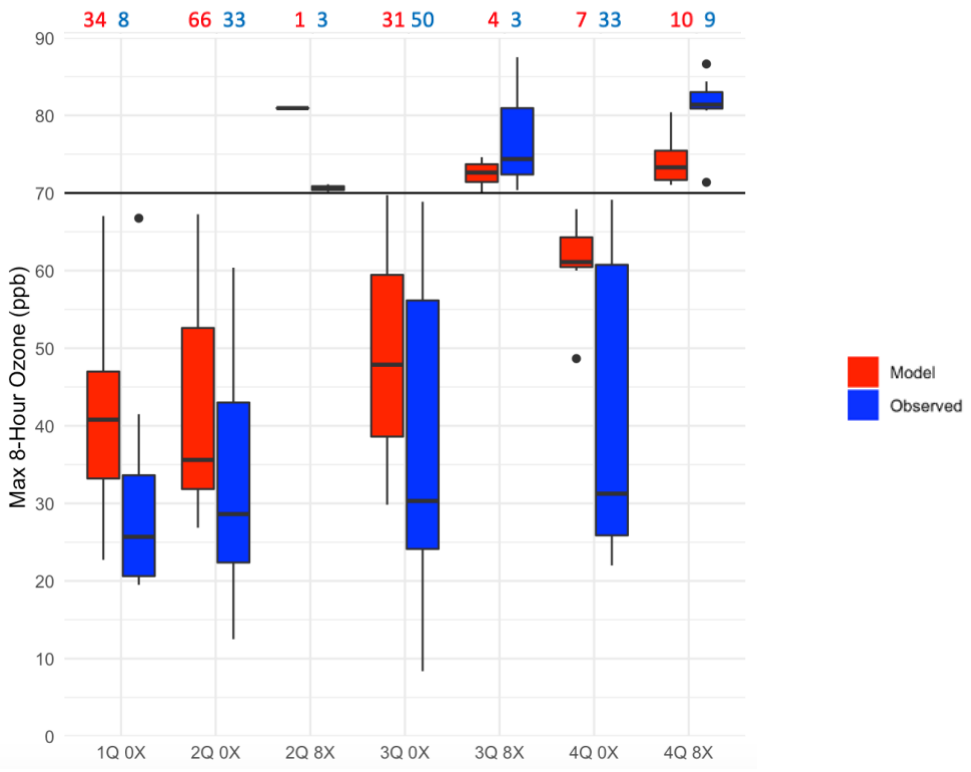

Figure 7. Boxplots for monitor Manvel Croix Park (MACP) predicted and observed max 8-hour ozone separated by quadrant and exceedance. These quadrants(1Q-4Q) coincide with the number of compass 90-degree quadrants the wind vector originated from between midnight to the following midnight (N:E, E:S, S:W, W:N). 8X days are days with O3 8H>= 70 ppb and 0X days are days with O3 8H< 70 ppb. Red and blue numbers represent the number of days within that quadrant and exceedance type.

Morning Wind Speeds

Figure 8 shows predicted and observed morning transport distances for all monitors. The observed morning transport distances only reach up to 80 km while the model predictions predict distances over 120 km. When observed transport distances are less than 20 km the predicted morning transport distances reach distances up to 100 km. It is apparent that for all monitors morning transport distance is consistently overpredicted due to the consistently faster wind speeds during those morning hours. There was also a spatial gradient in transport distances where the coastal monitors showed the largest overprediction of morning transport distances while monitors further west had the smallest overprediction. Figure 9 shows the morning

transport distances with O_3 concentration and wind rotation for coastal monitors, LJKS and SBFP. The morning transport distance is overpredicted for both LJKS and SBFP. While the observations show a large number of days occurring with morning transport distances less than 25 km the model rarely predicts days with morning transport distances less than 25 km. For both coastal monitors, the model predicts majority of days having morning transport distances over 50 km which is rarely seen in the observations. The majority of the LJKS monitor observed exceedances occurred with morning transport distances below 25 km. The model failed to predict high O_3 at these morning transport distances. Only one exceedance was predicted with a morning transport distance less than 25 km. The model predicted exceedances occurring with morning transport distances up to 73 km, which was never observed. The observations for the SBFP monitor also showed exceedance days occurring when morning transport distances were below 25 km which the model failed to predict. The model only predicted 2 days with morning transport distances below 25km and both days were non-exceedance days.

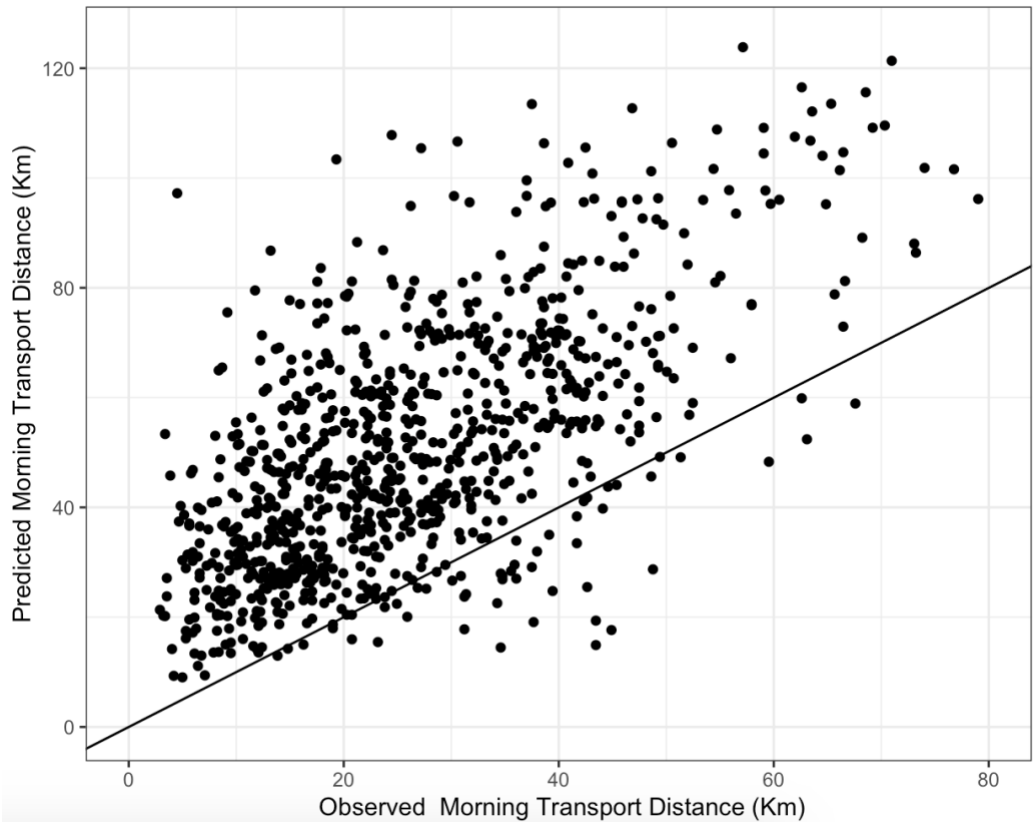

Figure 8. Predicted and observed morning transport distances (from hours 00:00 to 06:00) for all monitors. The reference line depicts where observed and predicted transport distances are equal.

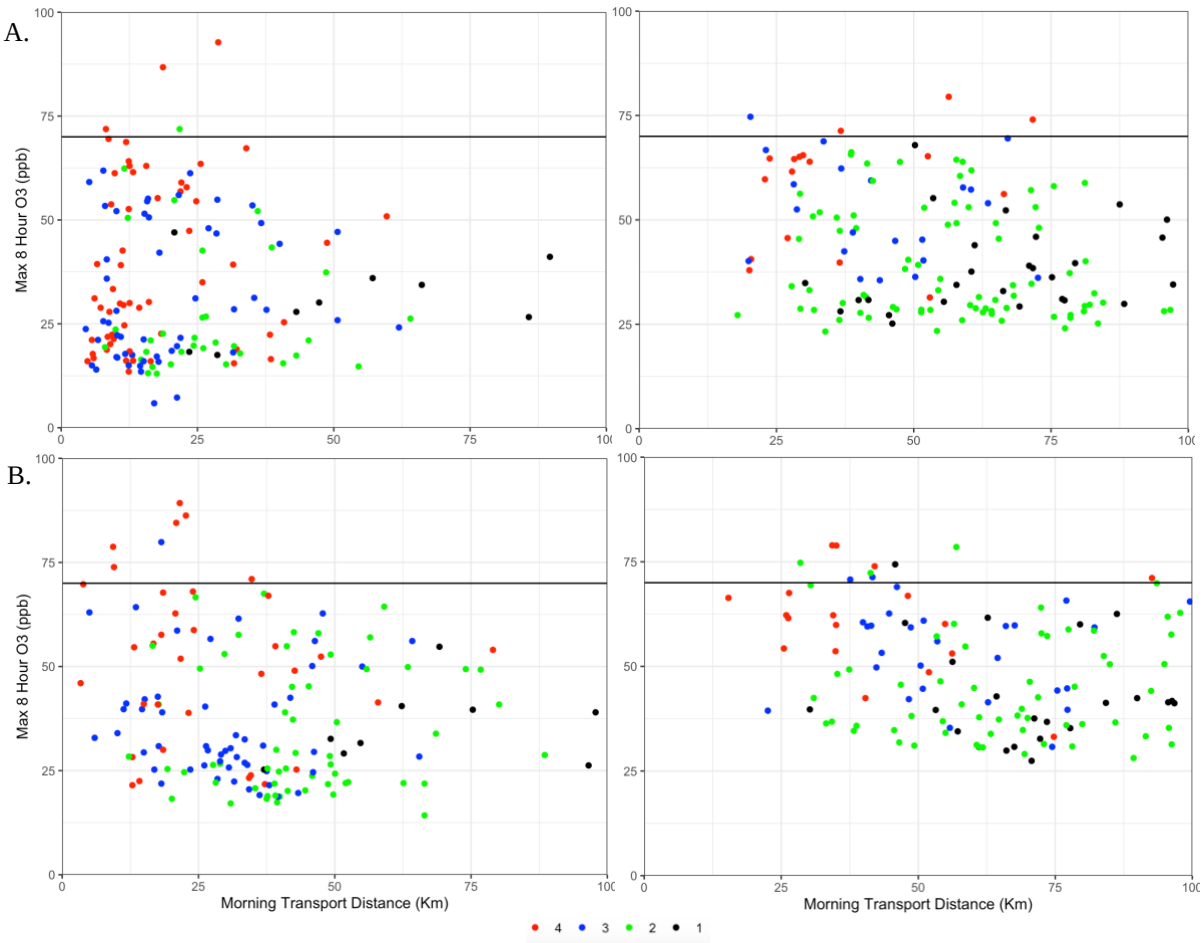

Figure 9. For monitors, (A) Lake Jackson (LJKS) and (B) Seabrook Friendship Park (SBFP), monitors daily maximum 8-hour ozone, morning transport distance, and quadrant type for the 153-day modeling period of May to September for (left) observed versus (right) predicted. Different colored dots represent the quadrant type graphed according to the morning transport distance for the daily maximum 8-hour ozone.

Both coastal monitors have the highest observed O_3 days occurring during 4Q days at transport distances less than 25 km (Figure 9). Model predictions for the LJKS monitor show majority of high O_3 days occurring on 4Q days but at morning transport distances over 25 km. The SBFP monitor model predictions had highest O_3 days occurring at all quadrants with morning transport distances over 25km. When looking at quadrant type in regard to morning transport distances and exceedances, the model failed to capture the patterns seen in the observations. Both monitor observations show patterns of high O_3 occurring during 3Q and 4Q days and low O_3 occurring throughout all quadrants. This is dissimilar from the monitor

predictions which both show high O_3 occurring on 3Q and 4Q days and low O_3 occurring on only 2Q and 1Q days. The observed 4Q day maximum 8-hour O_3 ranges were 11 to 100 ppb while the model predictions ranges were 32 -77 ppb. The model also predicted all maximum 8-hour O_3 concentrations to be between 25 and 88 ppb for both monitors while observational ranges were 6 to 90 ppb. The model predictions do not replicate the range of O_3 concentrations that occur day to day both overall and within quadrants. Altogether, when looking at monitor observations and model predictions, there is constant overprediction of morning transport distances, failure of predicting consistent high O_3 days within the right quadrants and failure to predict low O_3 days within all quadrants.

Figures 10 and 11 show the daily maximum 8-hour O_3, morning transport distance, and quadrant type for the inland monitors; MACP, DPK2, BAYP, and HALC. All inland monitor observations show majority of max 8-hour O_3 days occurring when the morning transport distance is below 25 km. In contrast, the model frequently predicted the majority of max 8-hour O_3 days occurring between morning transport distances of 25- 75 km. Monitor observations showed that as the morning transport distance increased, the number of O_3 exceedance days decreased. Yet, the model showed exceedance days occurring at all morning transport distances, even at transport distances over 50 km. Model predictions for MACP and DPK2 monitors show around half of the max 8-hour O_3 days occurring when morning transport distances are above 50 km, this is rare in the observations as most observed morning transport distances are below 50 km. All monitors have predicted days with morning transport distances reaching 100 km which is never seen in the observations; between all the monitors there is only one observed instance of morning transport distance being over 75 km. Days with morning transport distances less than 25

km were more frequent for monitors further inland. Nevertheless, all monitors show a constant overprediction of morning transport distances.

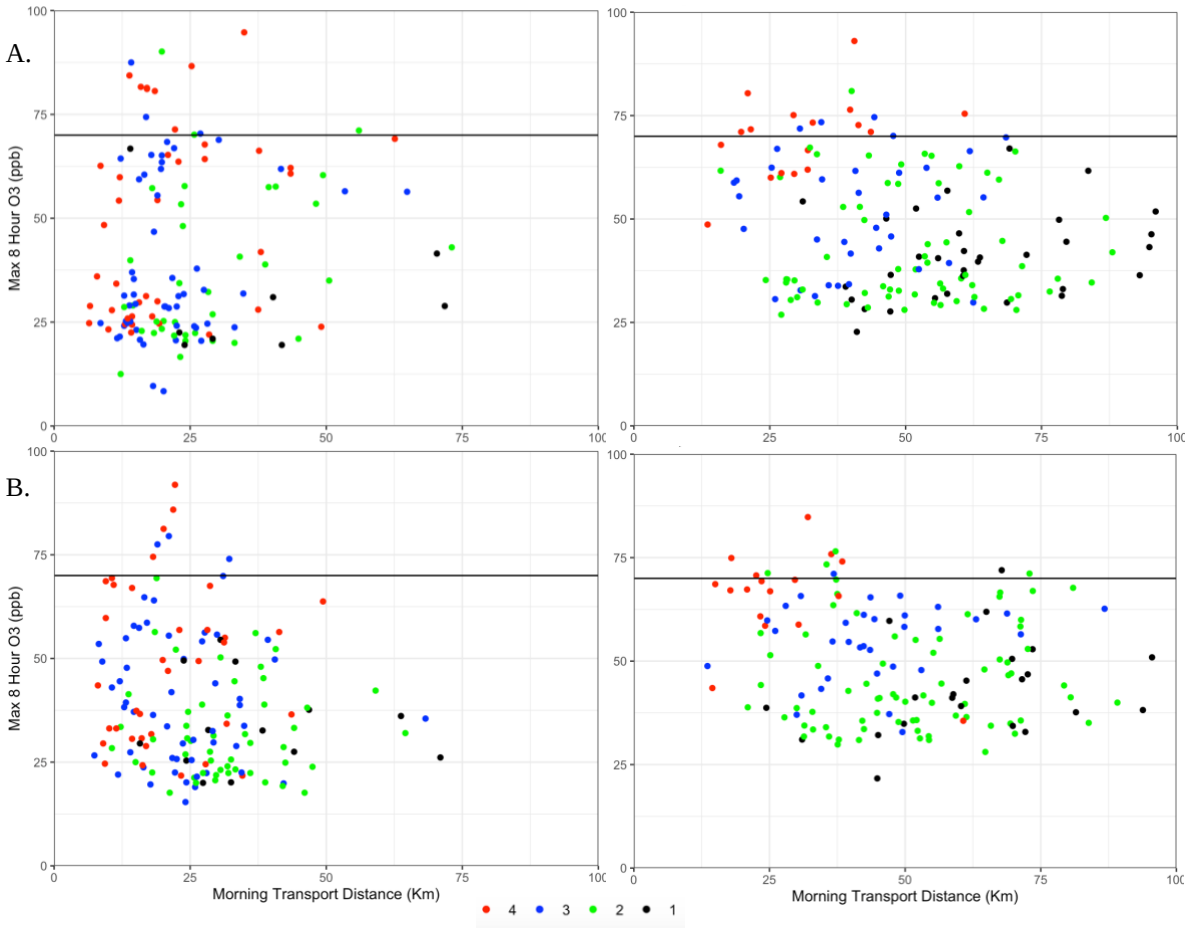

Figure 10. For monitors, (A) Manvel Croix Park (MACP) and (B) Deer Park #2 (DPK2), monitors daily maximum 8-hour ozone, morning transport distance, and quadrant type for the 153-day modeling period of May to September for (left) observed versus (right) predicted. Different colored dots represent the quadrant type graphed according to the morning transport distance for the daily maximum 8-hour ozone.

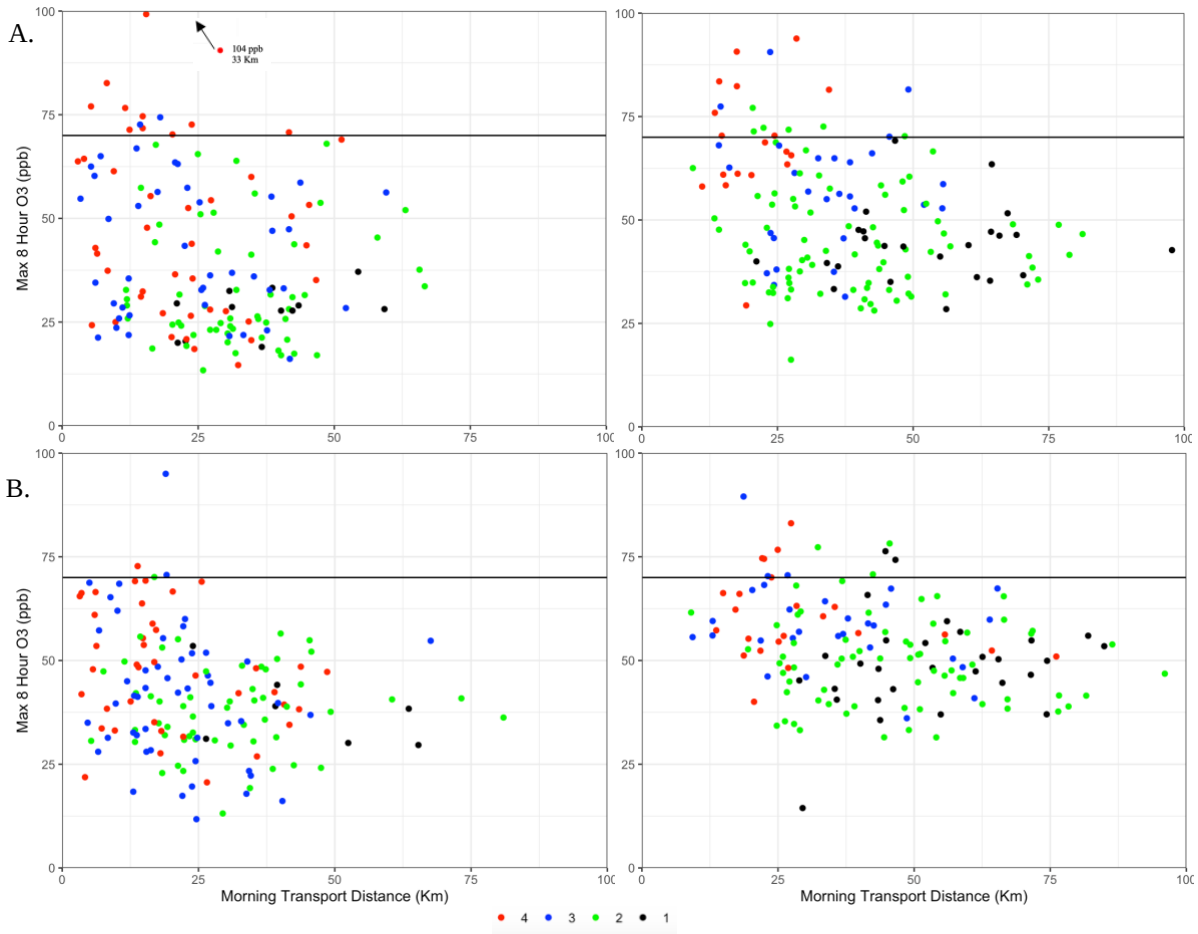

Figure 11. For monitors, (A) Bayland Park (BAYP) and (B) Aldine (HALC), monitors daily maximum 8-hour ozone, morning transport distance, and quadrant type for the 153-day modeling period of May to September for (left) observed versus (right) predicted. Different colored dots represent the quadrant type graphed according to the morning transport distance for the daily maximum 8-hour ozone.

Observed exceedances occurred most often during 3Q or 4Q days with morning transport distances less than 25km. While the model predicted the majority of exceedance days occurring during 3Q or 4Q days it failed to replicate the pattern of exceedances occurring when morning transport distances were low. Observed BAYP and HALC monitor 4Q days had max 8-hour O_3 concentrations between 25- 100 ppb while the model predicted majority 4Q days had max 8-hour O_3 concentrations over 50 ppb. The observed BAYP and HALC monitor 3Q days had max 8-hour O_3 concentrations as low as 10 ppb which was not seen in the model's predictions. In

comparison to MACP and DPK2 the model did a better job at replicating the pattern of exceedance days occurring on 3Q and 4Q days with lower morning transport distances. Despite this, the model still predicted various exceedance days occurring on quadrants and morning transport distances which were never observed. Between the two monitors there are only 2 observed instances of exceedance days occurring with morning transport distances over 25 km. In contrast, the model predicted various exceedance days occurring at morning transport distances over 25km. For both monitors, the observed 4Q max 8-hour O_3 concentrations ranged from 12-100 ppb. The model failed to capture this large range and had most 4Q days having max 8-hour O_3 concentrations over 50 ppb. The model also predicted most max 8-hour O_3 concentrations to be over 35 ppb when observations regularly showed max 8-hour O_3 concentrations below 25 ppb. Although the model does a better job at modeling the monitors further inland, the overprediction of morning transport distances and occurrence of exceedance days on quadrants and morning transport distances that are not observed persists. For all six monitors analyzed, the model fails to replicate multiple patterns seen in the observations and most importantly, the model fails to replicate the accurate morning transport distance that may lead to high O_3.

Midnight Wind Direction

Figure 12 shows the 0 LST wind directions as 90-degree sections which correspond to compass directions (NE, SE, SW, and NW) for coastal monitors. Coastal monitors showed majority of observed non-exceedance days occurring with midnight winds from the south. The model predicted majority of non-exceedance days occurring on SE 1Q or SW 2Q days while observations showed a larger variation of quadrants. Although the predicted midnight wind

directions for both coastal monitors also showed the majority of non-exceedance days coming from the south, the quadrants were incorrectly predicted. The observed LJKS midnight wind directions showed a substantial number of days with midnight winds from the NW which the model failed to reproduce. All observed exceedance days for the LJKS monitor had midnight wind directions from the NW which the model failed to predict. The majority of SBFP exceedance days occurred when the midnight wind direction came from the NW or SW. The model on the other hand, predicted exceedance days with all midnight wind directions but NE. By comparing observations to model predictions, it is apparent that both exceedance day and non-exceedance day midnight wind directions are rarely predicted correctly suggesting that the model creates fictional midnight wind directions for most if not all days.

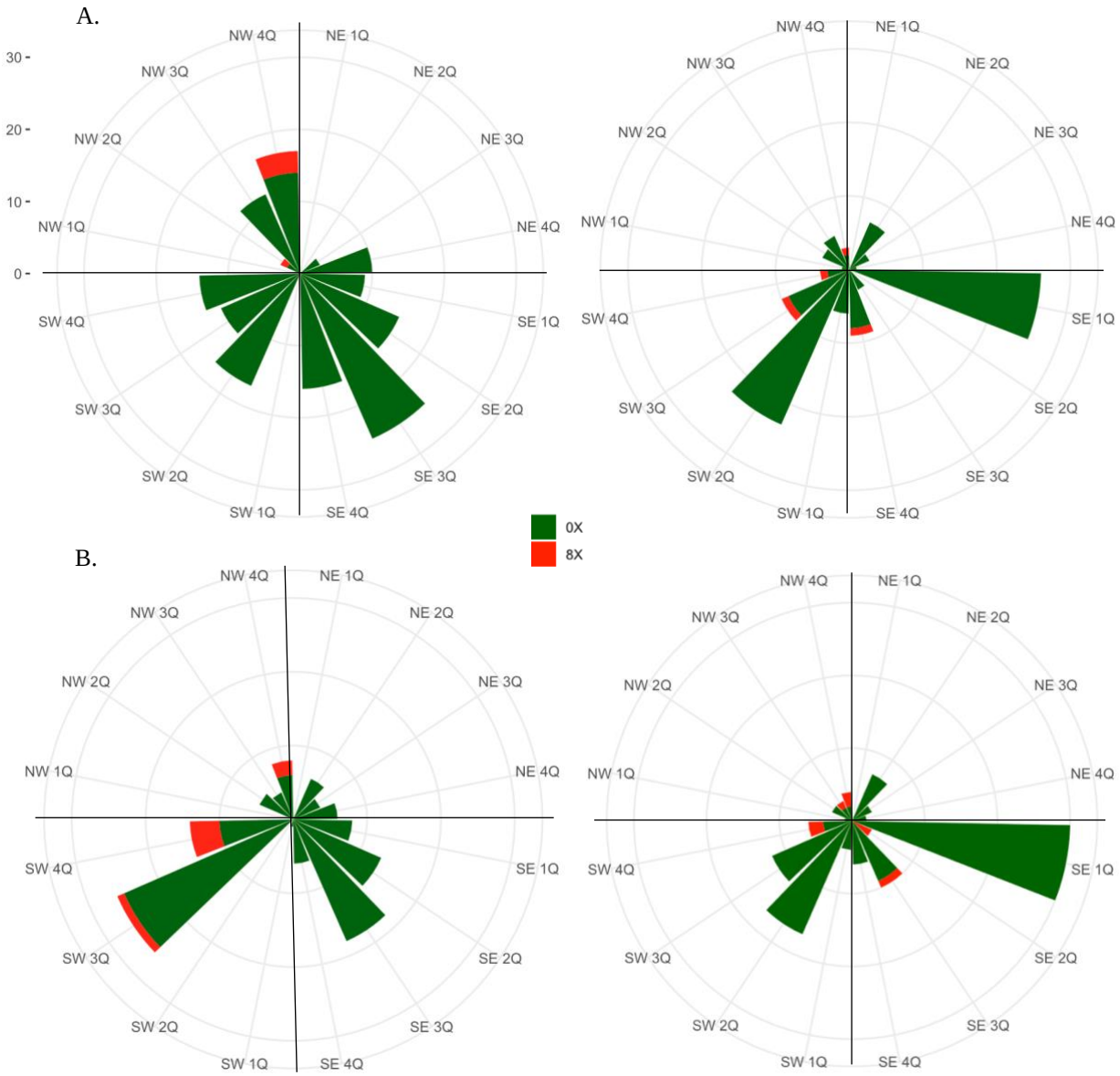

Figure 12. For monitors, (A) Lake Jackson (LJKS) and (B) Seabrook Friendship Park (SBFP), midnight winds, daily wind quads, and ozone exceedances for the 153-day modeling period of May to September for observed (left) versus predicted (right). These 90-degree sections correspond to compass directions and the rings represent number of days. The quadrants marked around the plots correspond to the same quadrants described in Figure 3.

Figure 13 shows the midnight wind directions for MACP and DPK2 and Figure 14 for BAYP and HALC. All inland monitors have majority observed non-exceedance days occurring from the south direction. While observations show non-exceedances from the south occurring for all quadrants, the model predicts non-exceedance days to be majority SE 1Q or SW 2Q days

which is not seen in the observations. Non-exceedance day predictions show overprediction of these SE 1Q and SW 2Q days and underprediction of all other days. While the observations show 4Q days with winds from the NW, NE, and SW directions as majority non-exceedance days with a few exceedance days, the model predicts the opposite (majority exceedance days with a few non-exceedance days). A consistent under prediction of non-exceedance days with NW-NE midnight wind directions was seen for both BAYP and HALC monitors. Altogether, the model failed to replicate the number of non-exceedance and exceedance days seen for all wind directions and quadrant types.

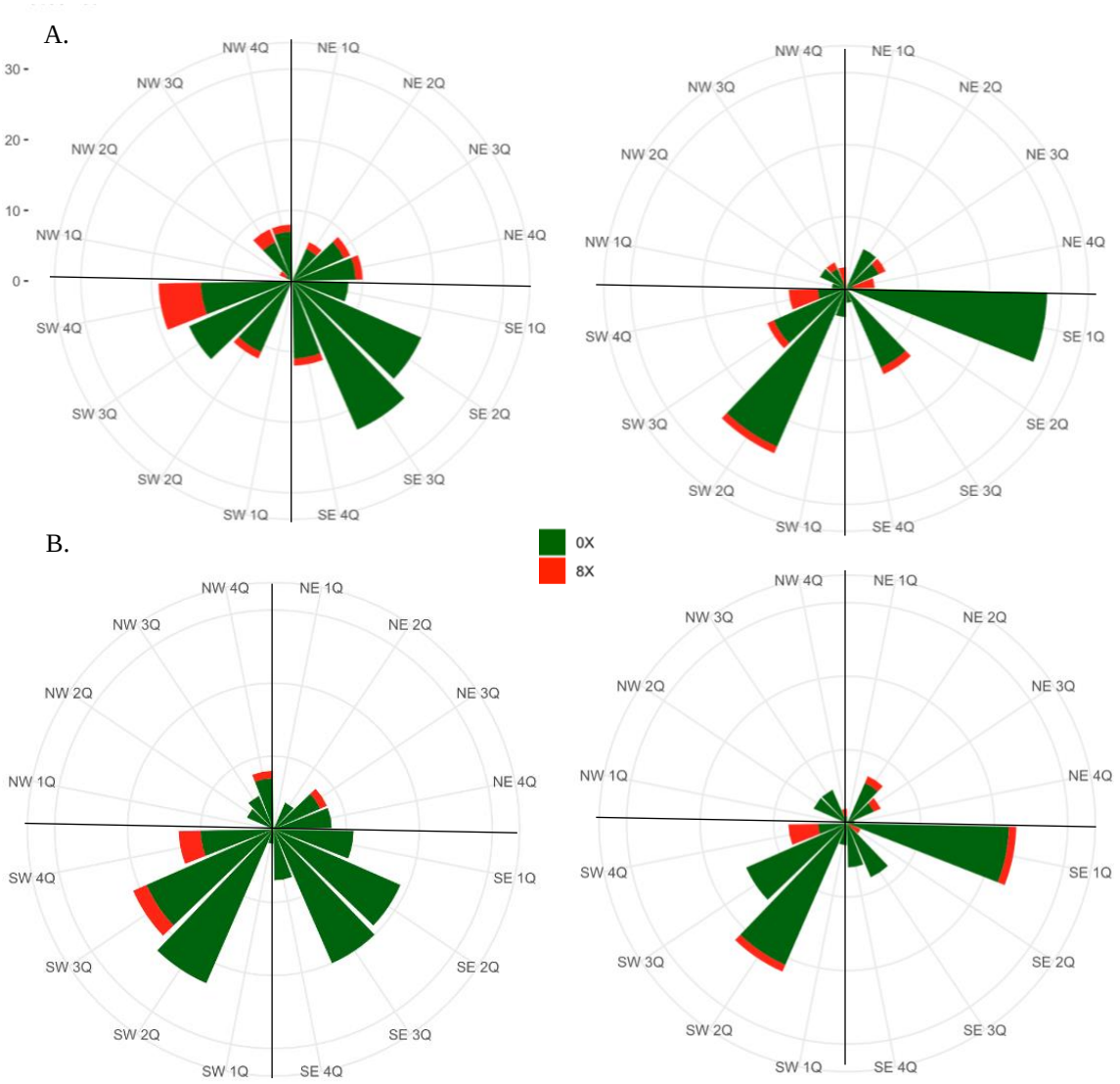

Figure 13. For monitors, (A) Manvel Croix Park (MACP) and (B) Deer Park #2 (DPK2) midnight winds, daily wind quads, and ozone exceedances for the 153-day modeling period of May to September for observed (left) versus predicted (right). These 90-degree sections correspond to compass directions and the rings represent number of days. The quadrants marked around the plots correspond to the same quadrants described in Figure 3.

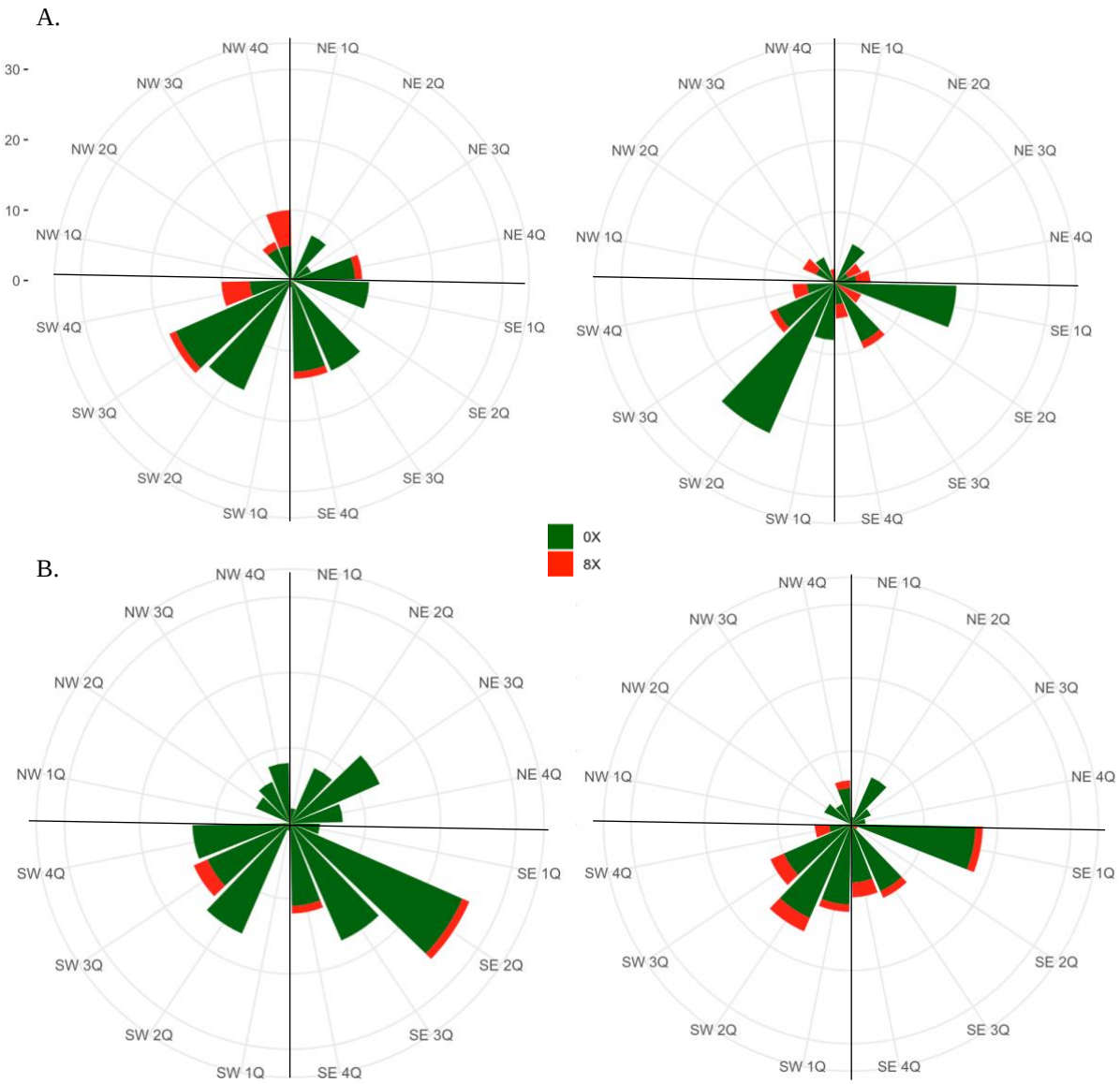

Figure 14. For monitors, (A) Bayland Park (BAYP) and (B) Aldine (HALC) midnight winds, daily wind quads, and ozone exceedances for the 153-day modeling period of May to September for observed (left) versus predicted (right). These 90-degree sections correspond to compass directions and the rings represent number of days. The quadrants marked around the plots correspond to the same quadrants described in Figure 3.

The MACP monitor model predictions and observations showed exceedances occurring at all midnight wind directions. The model correctly predicted the presence of 3Q and 4Q exceedances with midnight winds from the SW, NW and NE but failed to predict the correct number of exceedance days. Despite predicting the presence of some exceedance days correctly

for the MACP monitor, the model still consistently predicted exceedances occurring on quadrants where no exceedance was seen. The observed exceedance days for the DPK2 monitor occurred mostly when midnight winds came from the SW. The model also showed majority of exceedances occurring when winds came from the SW but failed to predict the accurate number of days and quadrants. Similar to the MACP monitor predictions, the model also predicted various exceedances occurring on quadrants and directions that showed no observed exceedances for the DPK2 monitor. The BAYP monitor had the majority of observed exceedances happening when midnight winds came from the SW-NW yet the model had numerous exceedances occurring at all midnight wind directions. As for the HALC monitor, exceedances were observed with midnight winds from the SW-SE. While the model did capture all but one predicted exceedance occurring from the SW-SE, it failed to predict the frequency and the quadrants these exceedances occurred on. Essentially, it is rare for the model to predict the quadrant, direction and number of days accurately. When considering all monitor's midnight wind directions in relation to exceedances and quadrants, the model fails to replicate patterns seen in the observations and predicts numerous days with midnight wind directions and quadrants that are not observed.

Exceedance Case Study: Unique meteorology

From the model evaluation, it is evident that while the majority of exceedance days are during 3Q or 4Q days the model continues to predict exceedance days during 2Q days. The model predicted 13 2Q exceedance days, of which only 1 was predicted correctly. Figure 15 shows the hourly O_3 concentrations for a day that is representative of an incorrectly predicted 2Q exceedance day. On this day, the predicted 2Q exceedance occurred for two monitors: SBFP and

DKP2. The winds start from the east and slowly curve towards the northwest. The high O_3 is widespread throughout the HGB area and the exceedances occurred on the edge of the regional high O_3 plume as shown in panel 2. As the day progresses the high O_3 moves towards the northwest similar to the wind direction. For this day at the DPK2 monitor location, the model predicted max 1-hour O_3 to be 81.1 ppb at 13:00 LST and for the SBFP monitor location the model predicted max 1-hour O_3 was 82.3 ppb at 17:00 LST (Supplemental Figures 4 and 5). Conversely, the observed highest O_3 concentrations were between 62-64 ppb at 13:00 LST for the DPK2 monitor and at 15:00 LST for the SBFP monitor. As seen in Supplemental Figures 4 and 5, the model is consistently overpredicting O_3 levels for these monitors. The morning transport distance was overpredicted by 10 km for both monitor locations. Midnight wind direction was predicted correctly, SE. The observed quadrant days were 3Q for SBFP and 4Q for DPK2, making the wind rotation incorrectly modeled. On this day there was only a slight wind rotation and the wind displacement was larger which rarely results in an observed exceedance. While these incorrectly predicted 2Q monitors were on the edge of the large regional O_3 plume, it is useful to know how the model predicted O_3 for a monitor within the highest band of O_3. The 8-hour max O_3 for the monitor where the highest O_3 was predicted, BAYP, was 92 ppb while the observations showed 8-hour max O_3 being only 72 ppb. This shows there was overprediction of O_3 occurring throughout the whole region. The wind rotation was also incorrectly predicted for the BAYP monitor, as the observations showed a 4Q day occurring for the BAYP monitor while the model predicted at 3Q day at this monitor.

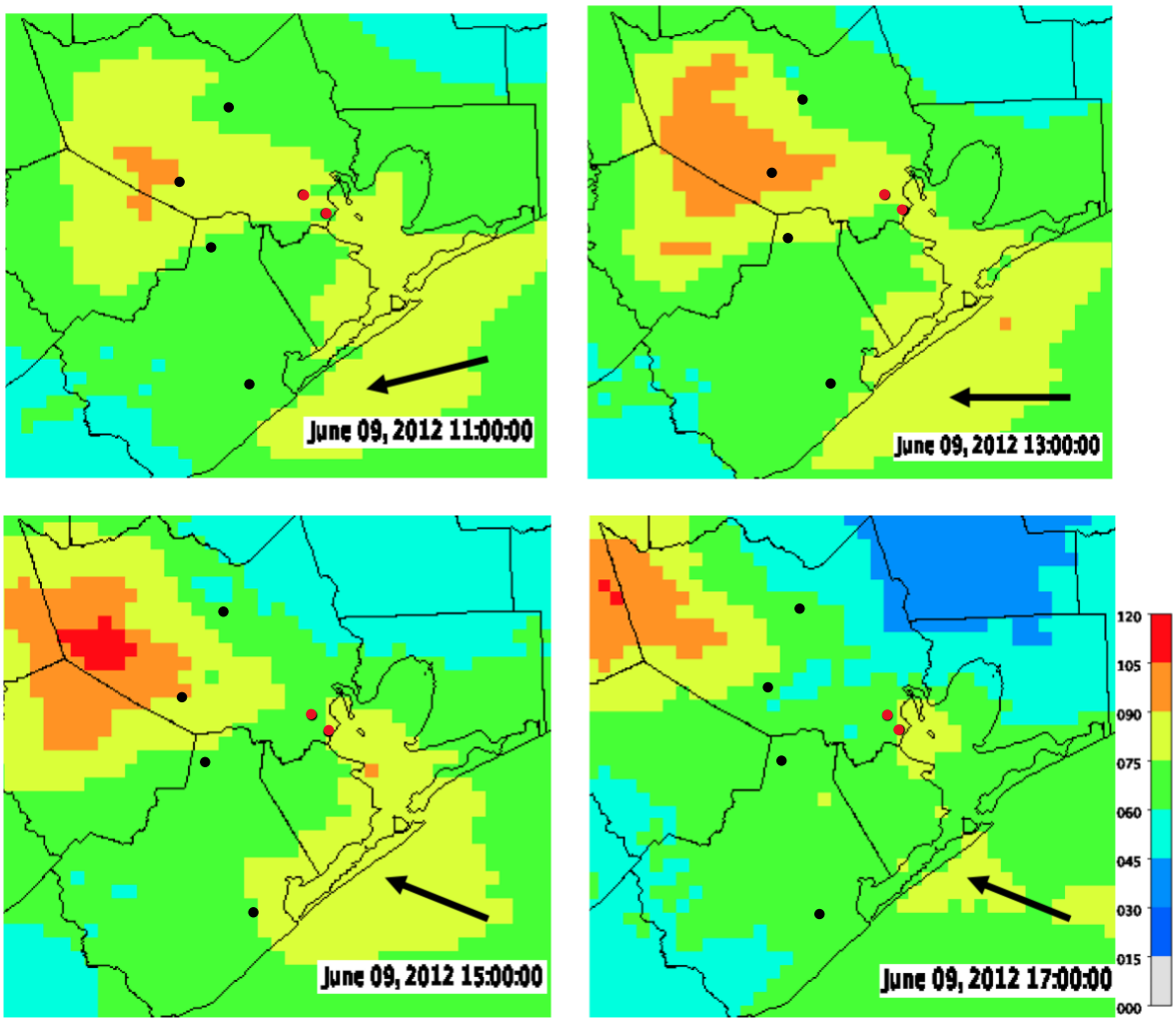

Figure 15. Modeled ozone concentrations (ppb) for the day June 9th at time points 11:00, 13:00, 15:00 and 17:00 local standard time (LST). On this day the model predicted 2Q exceedances which were not observed for the Seabrook Friendship Park (SBFP) and Deer Park #2 (DPK2) monitors (red dots). The black dots show locations of all other monitors used in this study. The arrows represent wind direction and displacement.

The one day that the model accurately predicted a 2Q exceedance is shown in Figure 16. The exceedance occurred at one monitor: MACP. Throughout the day the winds blew from the west and turned towards the southeast with less wind displacement than the wrongly predicted 2Q exceedance day. Again, the high O_3 was widespread throughout the HGB area and the ozone moved inland and then turned back into the coast. The model showed the highest O_3 concentration, 91.6 ppb, occurred at 15:00 LST. The time of highest O_3 concentration was

predicted correctly but the concentration was underpredicted by ~10 ppb (Supplemental Figure 6). Supplemental Figure 6 shows the underprediction of high observed O_3 for the MACP monitor. The morning transport distance was overpredicted by 10km for this monitor location as well and the midnight wind direction was predicted correctly, SW. Wind rotation was predicted correctly for this day as well, as both the model and observations showed a 2Q day occurring. The correctly predicted 2Q day has similar characteristics which demonstrate when an exceedance day would occur. In this case, the correctly predicted 2Q exceedance day was an instance when the winds created a rotation within 2 quadrants rather than 4 making an exceedance day occur.

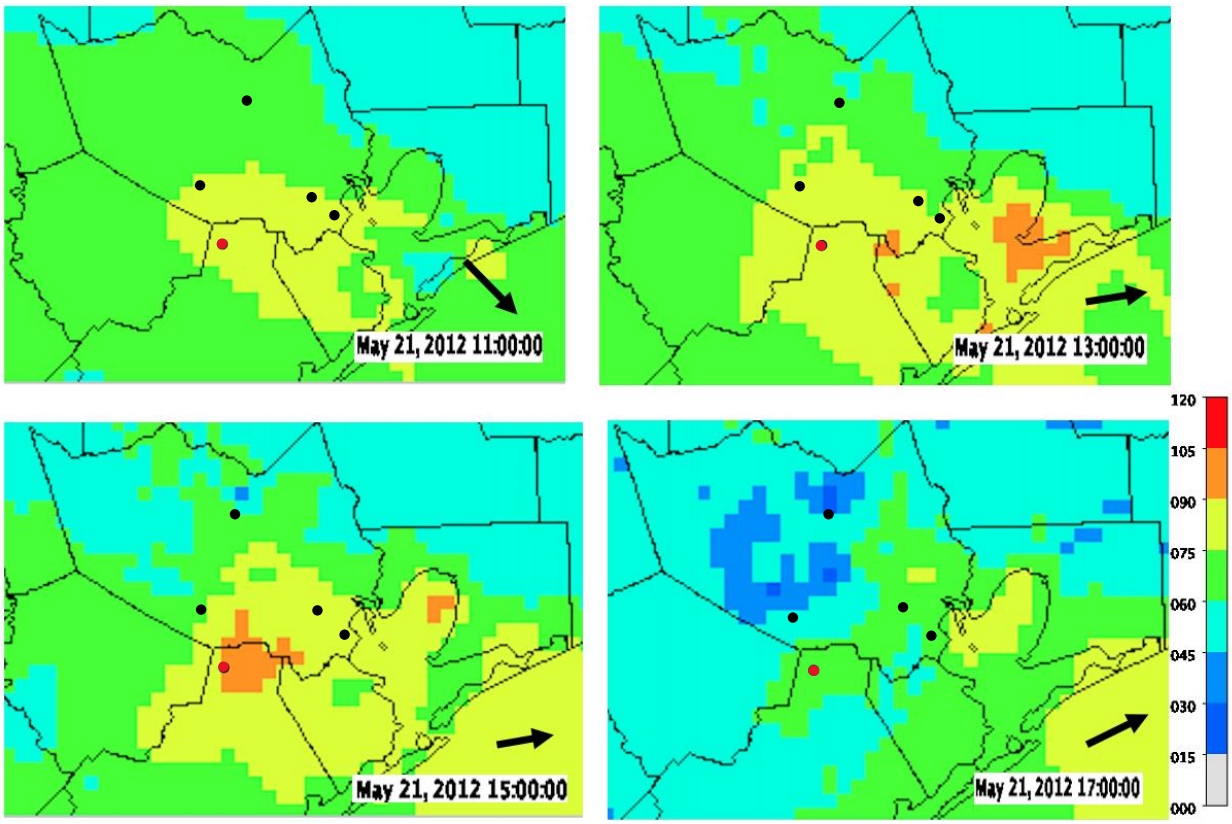

Figure 16. Modeled ozone concentrations (ppb) for the day May 21st at time points 11:00, 13:00, 15:00 and 17:00 local standard time (LST). On May 21st the model correctly predicted a 2Q exceedance for the Manvel Croix Park (MACP) monitor (red dot). The black dots show locations of all other monitors used in this study. The arrows represent wind direction and displacement.

CONCLUSION

This study quantifies the degree by which the HGB regulatory AQM is correctly simulating the meteorological processes that have been observed with O_3 exceedances. The regulatory AQM frequently underpredicted the full rotation of winds and tended to have higher wind speeds. An underprediction of wind rotation and overprediction of wind speed would normally be correlated with greater dilution and therefore lower O_3 but the opposite was observed. This may be due to compensating errors as it is evident that high O_3 continues to be predicted within the HGB area despite increased winds. These errors could include the incorrect modeling of the planetary boundary level (PBL) height or rate of emissions of precursors.

Houston's regional AQM uses the WRF model to create meteorological inputs and relies on the Yonsei University (YSU) scheme for vertical mixing (TCEQ, 2020b). A previous study in Houston analyzed surface level O_3 and various PBL schemes through the use of the WRF chemistry model (Cuchiara et al., 2014). Errors in these schemes included lower PBL height than observed in the nighttime and higher PBL height than observed in the daytime. These known errors could contribute to these compensating errors. In addition to vertical mixing, emissions in Houston have been a challenge. Studies have noted that NO_x emissions around the Houston Ship Channel tend to be overpredicted by 60% (Cuchiara et al., 2014; Kim et al., 2011). Choi et al. (2014) also found that Houston's NO_x emissions were overpredicted (> 10 ppb) but showed that the overprediction of O_3 cannot solely be attributed to the incorrect NO_x emissions (Choi, 2014). Finally, volatile organic compound (VOC) emissions from the oil and gas industry and flares

could also be a source (Murphy & Allen, 2005; Pavlovic et al., 2012). Highly reactive volatile organic compounds (HRVCOs) can cause O_3 to form rapidly within plumes containing industrial emissions from oil and gas companies (TCEQ, 2016). Overprediction of emissions or incorrect emissions are a few examples of possible compensating errors that may be occurring within the model causing high O_3 to be predicted despite the overprediction of winds. Attempting to reduce O_3 by creating control strategies based on a model with compensating errors could lead to ineffective strategies.

As seen in the quadrant analysis, observed quadrant types varied based on geographical location while predicted quadrants rarely showed geographical variation. This may mean that the model's 4 km grid cell resolution is insufficient to reproduce Houston's meteorological conditions. Previous studies have found that the largest impacts of model resolution on O_3 were associated with meteorological conditions and transport processes (Hodnebrog et al., 2011; Tie et al., 2010). This suggests that it is important to have an appropriate model resolution that is able to reproduce meteorological parameters that lead to accurately predicted O_3 concentrations. Recently, a study found that in regards to meteorology, finer grid resolution showed better reproduction of wind speeds and meteorological conditions in general (Tao et al., 2020). Increasing the resolution of the HGB regulatory AQM could prove to be beneficial to reproduce meteorological conditions that lead to peak O_3 concentrations.

In the absence of improved meteorology, the EPA model attainment demonstration allows for consideration of model performance through the use of a relative response factor (RRF). The RRF is the ratio of the future case average 8-hour daily maximum concentration predicated at a monitor to the base case average 8-hour daily maximum concentration predicted at a monitor. To calculate the base case average 8-hour daily maximum, the EPA recommends

using the 8-hour daily maximum O_3 concentrations for the 10 highest predicted O_3 days of the base year modeling at the monitor location if they are greater or equal to 60 ppb (EPA, 2014). To calculate the future case average, the future year modeling 8-hour daily maximum O_3 concentrations on the same days as chosen for the base case average at the monitor location should be used. The RRF is a key element of the attainment process because it is this value that is multiplied by the monitors design value to determine the percent reduction in a future year. Including days that are unable to simulate these observed meteorological processes would add uncertainty to future O_3 reductions. It may be possible to better represent observed ozone changes using an RRF built from days that represent ozone conducive conditions. Future work should investigate the sensitivity of the RRF to selecting days based on meteorologic parameters like wind rotation, morning transport distance, and midnight wind direction.

REFERENCES

Banta, R. M., Senff, C. J., Alvarez, R. J., Langford, A. O., Parrish, D. D., Trainer, M. K., Darby, L. S., Michael Hardesty, R., Lambeth, B., Andrew Neuman, J., Angevine, W. M., Nielsen-Gammon, J., Sandberg, S. P., & White, A. B. (2011). Dependence of daily peak O3 concentrations near Houston, Texas on environmental factors: Wind speed, temperature, and boundary-layer depth. *Atmospheric Environment*, *45*(1), 162-173. https://doi.org/https://doi.org/10.1016/j.atmosenv.2010.09.030

Beven, K., & Freer, J. (2001). Equifinality, data assimilation, and uncertainty estimation in mechanistic modelling of complex environmental systems using the GLUE methodology. *Journal of Hydrology*, *249*(1), 11-29. https://doi.org/https://doi.org/10.1016/S0022-1694(01)00421-8

Choi, Y. (2014). The impact of satellite-adjusted NO_x emissions on simulated NO_x and O₃ discrepancies in the urban and outflow areas of the Pacific and Lower Middle US. *Atmos. Chem. Phys.*, *14*(2), 675-690. https://doi.org/10.5194/acp-14-675-2014

Cuchiara, G. C., Li, X., Carvalho, J., & Rappenglück, B. (2014). Intercomparison of planetary boundary layer parameterization and its impacts on surface ozone concentration in the WRF/Chem model for a case study in Houston/Texas. *Atmospheric Environment*, *96*, 175-185. https://doi.org/https://doi.org/10.1016/j.atmosenv.2014.07.013

Darby, L. S. (2005). Cluster Analysis of Surface Winds in Houston, Texas, and the Impact of Wind Patterns on Ozone. *Journal of Applied Meteorology*, *44*(12), 1788-1806. https://doi.org/10.1175/JAM2320.1

EPA. (2014). *Modeling Guidance for Demonstrating Attainment of Air Quality Goals for Ozone, PM2.5, and Regional Haze* Research Triangle Park, NC Retrieved from https://www.epa.gov/sites/production/files/2020-10/documents/draft-o3-pm-rh-modeling_guidance-2014.pdf

EPA. (n.d.-a). *Ground-level Ozone Pollution*. Retrieved March 7 from https://www.epa.gov/ground-level-ozone-pollution/ground-level-ozone-basics#:~:text=Breathing%20ozone%20can%20trigger%20a,leading%20to%20increased%20medical%20care%20

EPA. (n.d.-b, January 21, 2021). *Timeline of Ozone National Ambient Air Quality Standards (NAAQS)*. Retrieved March 8 from https://www.epa.gov/ground-level-ozone-pollution/timeline-ozone-national-ambient-air-quality-standards-naaqs

Hodnebrog, Ø., Stordal, F., & Berntsen, T. K. (2011). Does the resolution of megacity emissions impact large scale ozone? *Atmospheric Environment*, *45*(38), 6852-6862. https://doi.org/https://doi.org/10.1016/j.atmosenv.2011.01.012

Kim, S. W., McKeen, S. A., Frost, G. J., Lee, S. H., Trainer, M., Richter, A., Angevine, W. M., Atlas, E., Bianco, L., Boersma, K. F., Brioude, J., Burrows, J. P., de Gouw, J., Fried, A., Gleason, J., Hilboll, A., Mellqvist, J., Peischl, J., Richter, D., . . . Williams, E. (2011). Evaluations of NO_x and highly reactive VOC emission inventories in Texas and their implications for ozone plume simulations during the Texas Air Quality Study 2006. *Atmos. Chem. Phys.*, *11*(22), 11361-11386. https://doi.org/10.5194/acp-11-11361-2011

Li, W., Wang, Y., Bernier, C., & Estes, M. (2020). Identification of Sea Breeze Recirculation and Its Effects on Ozone in Houston, TX, During DISCOVER-AQ 2013 [https://doi.org/10.1029/2020JD033165]. *Journal of Geophysical Research: Atmospheres*, *125*(22), e2020JD033165. https://doi.org/https://doi.org/10.1029/2020JD033165

Murphy, C. F., & Allen, D. T. (2005). Hydrocarbon emissions from industrial release events in the Houston-Galveston area and their impact on ozone formation. *Atmospheric Environment*, *39*, 3785-3798. https://doi.org/10.1016/j.atmosenv.2005.02.051

Nam, J., Kimura, Y., Vizuete, W., Murphy, C., & Allen, D. T. (2006). Modeling the impacts of emission events on ozone formation in Houston, Texas. *Atmospheric Environment*, *40*(28), 5329-5341. https://doi.org/https://doi.org/10.1016/j.atmosenv.2006.05.002

Pavlovic, R. T., Al-Fadhli, F. M., Kimura, Y., Allen, D. T., & McDonald-Buller, E. C. (2012). Impacts of Emission Variability and Flare Combustion Efficiency on Ozone Formation in the Houston–Galveston–Brazoria Area. *Industrial & Engineering Chemistry Research*, *51*(39), 12593-12599. https://doi.org/10.1021/ie203052w

Simon, H., Baker, K. R., & Phillips, S. (2012). Compilation and interpretation of photochemical model performance statistics published between 2006 and 2012. *Atmospheric Environment*, *61*, 124-139. https://doi.org/https://doi.org/10.1016/j.atmosenv.2012.07.012

Tao, H., Xing, J., Zhou, H., Pleim, J., Ran, L., Chang, X., Wang, S., Chen, F., Zheng, H., & Li, J. (2020). Impacts of improved modeling resolution on the simulation of meteorology, air quality, and human exposure to PM2.5, O3 in Beijing, China. *Journal of Cleaner Production*, *243*, 118574. https://doi.org/https://doi.org/10.1016/j.jclepro.2019.118574

TCEQ. (March 4 2021). *Air Quality and Monitoring*. Retrieved March 7 from https://www.tceq.texas.gov/airquality/monops/air-mon

TCEQ. (2016). *Houston-Galveston Brazoria Attainment Demonstration State Implementation Plan Revision For The 2008 Eighthour Ozone Standard Nonattainment Area*. Retrieved from https://www.tceq.texas.gov/assets/public/implementation/air/sip/hgb/HGB_2016_AD_RFP/AD_Adoption/16016SIP_HGB08AD_ado.pdf

TCEQ. (2020a). *Dallas-Fort Worth Serious Classificiation Attainment Demonstration State Implementation Plan Revision For The 2008 Eight-Hour Ozone National Ambient Air Quality Standard*. Retrieved from https://www.tceq.texas.gov/assets/public/implementation/air/sip/hgb/hgb_serious_AD_2019/HGB_AD_SIP_19077SIP_AppendixC_adoption.pdf

TCEQ. (2020b). *Houston-Galveston Brazoria Serious Classification Attainment Demonstration State Implementation Plan Revision For The 2008 Eight-Hout Ozone National Ambient Air Quality Standard* Austin, Texas Retrieved from https://www.tceq.texas.gov/assets/public/implementation/air/sip/hgb/hgb_serious_AD_2019/HGB_AD_SIP_19077SIP_adoption_web.pdf

TCEQ. (2021). *Compliance with Eight-Hour Ozone Standard*. Retrieved August 31 from https://www.tceq.texas.gov/cgi-bin/compliance/monops/8hr_attainment.pl

Tie, X., Brasseur, G., & Ying, Z. (2010). Impact of model resolution on chemical ozone formation in Mexico City: application of the WRF-Chem model. *Atmos. Chem. Phys.*, *10*(18), 8983-8995. https://doi.org/10.5194/acp-10-8983-2010

Vizuete, W., Nielsen-Gammon, J., Dickey, J., Couzo, E., Blanchard, C. L., Breitenbach, P., Rasool, Q., & Byun, D. (In Press). Meteorological based parameters and ozone exceedances in Houston and other cities in Texas. *Journal of the Air & Waste Management Association*.